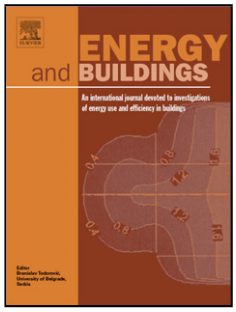

Title: Thermal impact of a redeveloped area on localized urban microclimate: A case study in Rome

Author: Gabriele Battista Emiliano Carnielo Roberto De Lieto Vollaro

PII: S0378-7788(16)31110-0
DOI: http://dx.doi.org/doi:10.1016/j.enbuild.2016.10.004
Reference: ENB 7063

To appear in: *ENB*

Received date: 13-4-2016
Revised date: 25-8-2016
Accepted date: 7-10-2016

Please cite this article as: Gabriele Battista, Emiliano Carnielo, Roberto De Lieto Vollaro, Thermal impact of a redeveloped area on localized urban microclimate: A case study in Rome, Energy and Buildings http://dx.doi.org/10.1016/j.enbuild.2016.10.004

Thermal impact of a redeveloped area on localized urban microclimate: A case study in Rome

Gabriele Battista[1,*], Emiliano Carnielo[1], Roberto De Lieto Vollaro[1]

[1]University of Roma TRE, Engineering Department, Via della Vasca Navale 79, Rome – 00146 Italy

*Corresponding Author: gabriele.battista@uniroma3.it

Abstract – The increase in urbanization leads to an intensification of the heat island effect, due to several factors: reduction in green areas; high solar absorptance of construction materials; waterproof surfaces; low sky view factors and natural ventilation effectiveness. Urban heat island characteristics have vast impacts and implications on energy efficiency, environment, and at last on human comfort and health. The development of urban fabric involves the modification of the thermal fluid-dynamic field of the whole area around the new buildings. This factor leads to worse the energy performances of all the structures affected by the phenomenon. The study investigates on the impact of a new building complex as result of a redevelopment process on the thermal and energy performances of the actual surrounding urbanized area sited in Rome. The purpose is to provide results to better understand the urban heat island effects on climate inside cities and population health. The assessment was carried out through a monitoring campaign and numerical analyses. The temperature field and the Universal Thermal Climate Index (UTCI) were calculated for the current scenario of the area, for the redeveloped configuration and for a proposed scenario characterized by the adoption of mitigation strategies against urban heat island countermeasures, such as vegetation improvement and cool materials able to limit the surface temperature rise under solar radiation.
The new redeveloped configuration of the area induces an increase in average air temperature up to 3.5 °C in the central part of the day and a worsening of the maximum UTCI index up to 2.7 °C. This is caused by the increase of the number of obstacle to the natural ventilation, the replacement of soil and spontaneous vegetation with low albedo materials. The application of cool materials and vegetation determines a temperature decrease up to 2 °C, while the maximum UTCI reduction is moderate, about 1 °C.

Keywords: Urban Heat Island; Universal Thermal Climate Index; ENVI-met; RayMan.

Nomenclature

d	index of agreement [-]
MAE	Mean Absolute Error [-]
MBE	Mean Bias Error [-]
N_D	number of analyzed data [-]
$\overline{O}$	mean of the observed variable
O_j	observed variables for each instant j
P_j	model-predicted variables for each instant j
RMSE	Root Mean Square Error [-]
SVF	Sky View Factor [-]
UTCI	Universal Thermal Climate Index [-]

1. Introduction

In 2009 the world energy outlook highlighted that most of EU population lives in cities [1]. The trend in new building designs are focused on the return of an investment without any evaluation of the possible worsening of the localized thermo-fluid dynamic conditions in energy and comfort terms. As a matter of fact, the buildings are obstacles to the natural ventilation inducing an increasing of hot air masses and polluting agents inside urban canyons.

Therefore, research on energy consumption and human health in urban areas are needed in order to reduce warming phenomena caused by the increase of urban density and the decrease of green areas. Although the urbanization has led to an increase in the global economy [2], the growing ratio of urban fabric on green areas lead to many environmental problems [3] both in micro and macro scale [4-8]. Liu et al. in 2005 [9] focused their attention on the correlation between the fast economy growth and the environmental issues affecting countries in Chinese territory. The main identified problems are pollution, biodiversity losses, cropland losses, depleted fisheries, desertification, disappearing wetlands and grassland degradation.

The environmental alteration caused by the urbanization led to the modification of the ecosystems [10,11]. In the last years there was an increase on the attention on the urban heat island (UHI) phenomenon. It is defined as the increase in urban areas temperature in comparison to the countryside adjacent to cities [12]. A Kolokotroni et al. study indicates that the urban heat island phenomenon is caused by microclimatic variations due to "manmade" intervention and modification of the natural environment [13].

Moreover, the UHI has effects on human health [14,15] and buildings energy performances [16-18] due to the thermo-fluid dynamic modification of air masses passing through urban structures [19,20].

In the last years, many studies aimed at assessing the impact of building energy consumption mitigation techniques on UHI, such as green roofs [21,22] and cool materials [23-26]. They are materials (paving, roofs and walls) characterized by a high solar reflectance and thus by surface temperatures sensibly lower than a conventional material; moreover, their high infrared emissivity value allows to emit and dissipate the stored heat towards the sky during night-time hours. A study of Carnielo et al. demonstrates how the increase in the reflectivity power of asphalt paving impacts on urban environment, reducing air temperatures and leading to a building energy consumption decrease during summer [27]. The use of cool materials technology combined with large green areas implementation leads to a sensible reduction of the urban heat island phenomenon [28].

Considering that in UE about 40% of total final energy consumption is attributed to civil sector, the need of devising new tricks acquires a new form in analyzing how passive energy-saving techniques can also induce sensible benefits in heat island mitigation by reducing the cooling demand and consequently the electricity demand during summer.

2. Objective and Methods

The need of improving the physical environment of a degraded and disused area in a popular district of Rome has led to design a new large commercial building complex. As reported in several studies [29-31], the increase in built surfaces will result in an alteration of the local climatic conditions of the whole nearby zone. This work shows a case study analysis with the aim of assessing the extent of this alteration and the possible thermal conditions mitigation associated to the use of urban heat island countermeasures applied on the area to be redeveloped. The paper is organized in two sections:

- *Monitoring campaign*: A measurement reference point was chosen within the disused area in order to collect microclimatic parameters. The measurement campaign was carried out during a summer day. The only purpose of the campaign is to extract sufficient data to validate the micro-scale models used in the numerical analyses;

- *Numerical Analyses*: A holistic microclimate tool able to simulate the variation of several thermal atmospheric parameters was used to model three 3D micro-scale urban configurations including the site to be redeveloped and the surrounding neighboring areas:

    1. The first model is based on the current conditions of the area. The input parameters of this model were opportunely changed in order to match the output results with the microclimatic data extracted from the monitoring campaign;
    2. The second 3D model recreate the future redeveloped scenario;
    3. A new configuration was proposed consisting of an alternative version of the previous model. It is characterized by cool materials applications and vegetation improvement within the original requalification project.

The outputs extracted from the simulations carried out on the three micro-scale models allows the study of temperature field over the whole investigated domain and the comparisons among the models. More specifically, temperature vertical profiles associated to an investigation point selected outside the area to be redeveloped were examined in order to quantify the influence on the surrounding environment thermal performances. Moreover, the temperatures profiles were used to extract a thermal comfort index calculated in the aforementioned point.

3. Case study description: "Ex Mercati Generali"

A disused group of buildings called "Ex Mercati Generali" is placed in Ostiense, a popular neighborhood extended in the southern part of the urban area of Rome at latitude 41.87 and longitude 12.48. The "Ex Mercati Generali", shown in Figure 1(a) enclosed in the yellow dot line, is an area of about 90,000 m^2 composed by 13 historical buildings with a height up to 8 meters. Currently, the area mainly consists of rubble, sandy soil and spontaneous vegetation. It is embedded in a mainly residential zone built in different periods. The actual prevalent typology is high rise buildings (30 meters) along a 60 meter wide boulevard with trees in between. The area is also characterized by large urban voids, mainly covered by asphalt (e.g. parking lots).The site taken into account in this study include the "Ex Mercati Generali" and the surrounding areas covering about 360,000 m^2.

4. Microclimatic measurement campaign

The monitoring campaign was carried out by means of a microclimatic station placed in the area at 6.5 m of elevation above the ground. Four weather parameters were measured:

1. Outdoor temperature:
2. Wind velocity;
3. Relative humidity;
4. Intensity of solar radiation on the horizontal plane.

Figure 1 shows the measurement point. The choice of this point was made to limit the influence of traffic on the measured quantities.
The climatic station is composed by a LSI Lastem M-Log data logger linked with a hot wire anemometer for the air velocity measurements and a psychrometer for the measure of air temperature and relative humidity. The solar radiation measurement was carried out by means of a Delta Ohm HD 2102.2 assembled with a pyranometer LP Pyra 03.The data of the aforementioned quantities were recorded from 9:00 AM to 4:00 PM on July 16th, 2014.

5. Calculation

The first part of the numerical analysis reported in this work was carried out with ENVI-met 4.0 [32]. It is a transient tool able to recreate urban 3D models based on a soil-vegetation-atmosphere transfer scheme realized with deterministic equations that couple thermal and fluid-dynamics processes. It is possible to edit thermal, optical and solar characteristics of the elements composing the model. Recent studies were based on ENVI-met calculations to predict thermo-physical phenomena in the urban environment, trying to match calculated parameters with measured ones [33-35].
ENVI-met requires to set in input several atmospheric quantities. The input values used in the proposed study are reported in the following Table 1. They are set as constants with the exception of atmosphere temperature parameter that was changed in order to perform the model validation process as will be described below.

The air temperature profiles extracted from ENVI-met simulations on July 16th were used as input to calculate the thermal comfort index UTCI (Universal Thermal Climate Index) based on an equivalent temperature concept. The software used for the calculation is RayMan [36,37], which is able to calculate human thermal comfort in urban areas. In the UTCI index, the meteorological conditions are compared to a reference environment, which has 50% relative humidity, calm air and the mean radiant temperature being equal the air temperature [38]. The UTCI equivalent temperature for a given meteorological condition is defined as the air temperature of the reference environment that produces the same physiological stress (strain) [39].

5.1. Model description

In Figure 2 the three 3D micro-scale urban model inputted in ENVI-met are presented. They are composed by a mesh of 126 x 115 x 30 square cells. Each cell has a dimension of 5(x) x 5(y) x 3(z) meters. Models differ in the central part, highlighted in yellow dots in Figure 2 (a), where three configurations of the "Ex Mercati" were implemented, while the nearby areas are modeled with same geometrical optical and thermal characteristics.
Figure 2(b) shows the current state area hereinafter called *ante-operam*. Figure 2(c) shows the designed redeveloped area hereinafter called *post-operam*. At last Figure 2(d) present the proposed configuration equipped with high solar reflectance materials, green roofs and extended gardens. This geometry will be called *final-post-operam*.

The following Table 2 reports the main thermal and solar properties of materials (soils and buildings) used in the urban models.

5.2. Model validation

Once the *ante-operam* model was put in the simulation tool, a validation process was performed by comparing the measured temperature data with numerical results by varying the initial potential temperature of atmosphere at 2500 m, in order to match it with the actual outdoor temperature peak, being equal the intensity of solar radiation peak and its daily distribution and having set a simulation date equal to the measurement date. As shown in Figure 3, an air temperature and relative humidity receptor was placed in the model in the corresponding point where the actual measurements were performed.

Different statistical indices were used to analyze the differences between the simulated and experimental data. Considering P_j and O_j respectively the model-predicted and observed variables for each instant j, N_D the number of analyzed data and $\overline{O}$ the mean of the observed variable, the quantitative indicators [40] adopted in this study are:

- The mean bias error (MBE). It indicates if the model values underestimates or overestimates the observed data. This indicator does not work correctly when an alternation of overestimations and underestimations of predicted values are registered, because they set off against each other.

$$\mathrm{MBE} = \frac{\sum_{j=1}^{N_D}(P_j - O_j)}{N_D} \tag{1}$$

- The Root Mean Square Error (RMSE). It is the standard deviation of the differences between predicted and observed values. It is worth to notice that few large errors led to a great RMSE value.

$$\mathrm{RMSE} = \sqrt{\frac{\sum_{j=1}^{N_D}(P_j - O_j)^2}{N_D}} \tag{2}$$

- The Mean Absolute Error (MAE). It is the same of the MBE indicator but it takes into account the absolute difference between predicted and observed values. For this reason, this indicator is useful when there are an alternation of overestimations and underestimations predicted values.

$$\mathrm{MAE} = \frac{\sum_{j=1}^{N_D}\left|P_j - O_j\right|}{N_D} \tag{3}$$

- The index of agreement "d". It is a statistical indicator that quantifying the agreements between predicted and observed values. With values ranged from 0 to 1, the index of agreement is usually used to cross-compare different models.

$$d = 1 - \left[\frac{\sum_{j=1}^{N_D}\left[\left(P_j - \overline{O}\right) - \left(O_j - \overline{O}\right)\right]^2}{\sum_{j=1}^{N_D}\left(\left|P_j - \overline{O}\right| + \left|O_j - \overline{O}\right|\right)^2}\right] = 1 - \left[\frac{\sum_{j=1}^{N_D}\left(P_j - O_j\right)^2}{\sum_{j=1}^{N_D}\left(\left|P_j - \overline{O}\right| + \left|O_j - \overline{O}\right|\right)^2}\right] \tag{4}$$

The following Figures 4, 5 and 6 show the assessment of the simulation error between the observed and the model-predicted air temperature and relative humidity values recorded in the RC point, varying the initial potential temperature of the atmosphere. Figure 4 shows the air temperature and humidity trend of the simulated and observed data. Figure 5 and 6 show the results of the statistical indices both for air temperature and humidity.

As inferred by the statistical analysis findings shown in Figures 5 and 6, the value of potential air temperature at 2500 m that results to be more in agreement with the data recorded with the microclimatic

station is 296 K. As a matter of fact, in Figure 4 the curve corresponding to an initial temperature of the atmosphere of 296 K can approximate the observed values. The Table 3 show the statistic index results for the initial temperature of the atmosphere equal to 296 K.

5.2. Temperature distribution: ENVI-met results

Figures 7, 8 and 9 show the temperature field at 1.5 m height above the ground, through a chromatic scale, on a horizontal plane on July 16th at 6:00 AM, 12:00 AM and 6:00 PM respectively. As expected, the comparison between *ante-operam* and *post-operam* (the redeveloped scenario) demonstrates as the increase in the built surfaces can significantly raise the air temperature value in the domain. The addition of surfaces absorbing the energy coming from solar radiation encourages the convective heat exchanges with air. The average values of air temperature variation are 2.5 °C at 6:00 AM, 3.5 °C at 12:00 AM, 3 °C at 6:00 PM.
The use of cool materials on vertical and horizontal surfaces and vegetation improvement in the *final-post-operam* model confirms to be effective in the mitigation of the outdoor environment temperatures. In fact, by comparing the *post-operam* model results with the ones obtained with the *final-post-operam* model, it is worth to notice an air temperature decrease of 0.5 °C at 6:00 AM, 2 °C at 12:00 AM and 1.5 °C at 6:00 PM. Despite the previous result, temperatures calculated for the *final-post-operam* model are still sensibly higher than those recorded in the *ante-operam*: the substantial increase of constructed surfaces does not allow an adequate air mixing impeding the transportation of warm air masses out of the domain.

Relevant results are obtained by observing Figure 11, where the vertical temperature profiles are displayed. The investigation point in which they were calculated is indicated in Figure 10. It is worth to notice as this point is placed outside the area to be rdeveloped, in a road intersection. Through the observation of these results it is possible to assess the thermal impact of the new built on the surrounding urban area.

The vertical temperature trends are different in shape, depending on the time of day when the profiles were extracted. In fact, at 6:00 AM the surface temperature of the ground is lower than the one of the air above it, due to a moderate solar irradiation in the early morning. On the other hand the vertical profiles at 12:00 AM and 6:00 PM denote an inverse behavior.
Passing from the *ante-operam* model to the more thermally critical *post-operam* model, the maximum temperature increase is registered at low heights, under the canopy (average buildings height), close to the ground: 1.6 °C at 6:00 AM; 2.3 °C at 12:00 AM and 2.7 °C at 6:00 PM. The new building complex worsens the thermal characteristics of the urban zone not only inside its borders but also in the adjacent area.
Again, the use of cool materials and vegetation proposed in *final-post-operam* model determines a decrease in temperature mostly under the canopy. By comparing the results with the ones obtained for the *post-operam* model the maximum temperature variations are: 0.6 °C at 6:00 AM (the solar radiation does not significantly influence the heat exchanges in early morning making the cool materials ineffective); 1.1 °C at 12:00 AM and 1°C at 6:00 PM. The benefits depending on the countermeasures are more effective under the canopy due to the favorable convective heat exchanges between surfaces and air, but they are also present over the canopy although they slightly decrease with height.

5.3.Estimating outdoor thermal comfort: RayMan results

Thermal stress is assessed with a 10 point scale shown in Table 4. UTCI temperature values are associated with a stress category comply closely with the definition assumed in the Glossary of Terms for Thermal Physiology in 2003 [41].

UTCI is calculated for the three urban models in the same chosen point previously described and shown in Figure 10. Hourly simulation results, extracted at 1.5 m height above the ground on July 16th, are presented in Figure 12. The UTCI permanence within the "no thermal stress" category is very similar for the three considered urban models: 54%, 46% and 50% of the day for the *ante-operam*, *post-operam* and *final-post-operam* respectively.
In the central part of the day, when solar irradiation reaches the highest values, more significant differences among the considered configurations are observed. UTCI remains in "strong heat stress" for 6 hours for the *ante-operam* while the figure amounts to 9 and 8 hours for the *post-operam* and *final-post-operam* respectively. The maximum in UTCI value is 34 °C for the *ante-operam* while it reaches a value higher than 37 °C for the *post-operam* model. However, these values are both contained within the "strong heat stress" category. The application of cool materials and vegetation improving in the area to be redeveloped (represented by the *final-post-operam* model) determines a modest decrease in the maximum UTCI value of about 1°C.

6. Conclusions

The study assesses the impact of new buildings on the localized microclimate conditions of a popular neighborhood of Rome. The purpose is to provide results to better understand the urban heat island effects on climate inside cities and population health. A case study was analyzed related to a disused area of 90,000 m^2 for which a redevelopment project is planned. Three 3D urban models were implemented: the first one called *ante-operam* represents the current conditions (a disused site); the second one called *post-operam* represents the renovated scenario, namely a multipurpose commercial center, characterized by a strong increase in the built surfaces; the third one called *final-post-operam* represents a proposed configuration consisting in the application of high solar reflectance materials and vegetation improvement in order to mitigate the localized urban heat island phenomena deriving from the presence of the new buildings. The findings show how the indiscriminate and poorly planned urbanization leads to the expected critical thermal issues due to high solar absorption and obstacles which do not allow air to freely circulate. Moreover, the effectiveness of urban heat island effect countermeasures applied in the case study is examined.

1. A thermal analysis was carried out with ENVI-met, a holistic microclimate tool able to recreate an urban portion with buildings and roads. Simulations results allow to analyze the horizontal distributions of average outdoor temperature calculated in a reference day (July 16th). The comparison between *ante-operam* and *post-operam* configurations in the central part of the day denotes an increase in average temperature of 3.5 °C. The application of cool materials and vegetation as urban heat island countermeasures leads to a decrease in average temperature of 2 °C, as inferred by the comparison between *post-operam* and *final-post-operam*.
2. Further information were found examining the vertical temperature distribution in an investigation point specifically chosen outside the area to be redeveloped. It allows to investigate the thermal and comfort conditions of the spaces surrounding the case study area as a function of the different chosen urban models. As expected, an increase in built surface mostly affects the localized microclimate conditions under the average height of buildings. In the *post-operam* configuration a maximum increase in temperature of 2.7 °C is registered at 6:00 PM close to the ground level with respect to the *ante-operam* configuration. The *final-post-operam* configuration determines a small decrease in temperature if compared to the *post-operam* with a maximum value of 1.1 °C reached at 12 AM. The differences in temperature between the *post-operam* and the *final-post-operam* become thinner increasing the height.
3. An outdoor comfort index, the Universal Thermal Climate Index (UTCI), was evaluated through the RayMan tool in the same reference point where the vertical temperature distributions were extracted. The daily permanence of UTCI under the "no thermal stress" category is very similar to the three urban model, ranging between 46 to 54% of the day. More significant differences among the models were found analyzing

the UTCI permanence inside the "strong heat stress" category occurring during the highest solar irradiation hours. In *post-operam* model UTCI remains confined in the category 3 hours more than in the *ante-operam* model with a maximum increase of 3 °C. Urban heat island countermeasures decrease by 1 hour the UTCI permanence in the "strong heat stress" category associated to a reduction of the maximum UTCI value of 1 °C.

As demonstrated in this study, the use of cool materials and vegetation integrated in a building complex is recommended and it leads to a decrease of the critical issues that give rise to the urban heat island phenomenon in the surrounding zones.

7. References

[1] International Energy Agency, World energy outlook 2008-2009, Geneva, 2008-2009

[2] A.De Sherbinin, A.Schiller, A.Pulsipher, The vulnerability of global cities to climate hazards, Environment and Urbanization 19(2007) 39-64.

[3] L.Cui, J.Shi, Urbanization and its environmental effects in Shanghai, China, Urban Climate 2 (2012)1-15.

[4] Y.H.Kim, J.J.Baik, Spatial and temporal structure of the urban heat island in Seoul, Journal of Applied Meteorology 44 (2005) 591-605.

[5] S.S.D.Foster. The interdependence of groundwater and urbanisation in rapidly developing cities, Urban Water 3-3 (2001) 185-192.

[6] B.Li, R.Yao, Urbanisation and its impact on building energy consumption and efficiency in China, Renewable Energy 34-9 (2009) 1994-1998.

[7] I.Martínez-Zarzoso, A.Maruotti, The impact of urbanization on CO2 emissions: evidence from developing countries, Ecological Economics 70-7 (2011) 1344-1353.

[8] G. Battista, T. Pagliaroli, L. Mauri, C. Basilicata, R. De Lieto Vollaro, Assessment of the Air Pollution Level in the City of Rome (Italy), Sustainability 8-9 (2016) 838.

[9] J.G.Liu, J. Diamond, China's environment in a globalizing world, Nature435 (2005) 1179-1186.

[10] J.E.González, J.C.Luvall, D.Rickman, D.Comarazamy, A.Picón, E.Harmsen, H.Parsiani, R.E.Vasquez, N.Ramirez, R.Williams, R.W.Waide,C.A.Tepley, Urban heat islands developing in coastal tropical cities, EOS, Transactions, American Geophysical Union 86-42 (2005) 397-398.

[11] M. Santamouris, D. Kolokotsa, Urban Climate Mitigation Techniques, first ed., Abingdon, UK, 2016.

[12] R.A. Memon, D.Y.C. Leung, C. Liu, An investigation of urban heat island intensity (UHII) as an indicator of urban heating, Atmospheric Research 94 (2009) 491-500.

[13] M. Kolokotroni, I. Giannitsaris, R.Watkins, The effect of London urban heat island on building summer cooling demand and night ventilation strategies, Solar Energy 80(2006) 383-392.

[14] D.Taleb, B.Abu-Hijleh, Urban heat islands: Potential effect of organic and structured urban configurations on temperature variations in Dubai, UAE, Renewable Energy 50 (2013) 747-762.

[15] K. Giannopoulou, I. Livada, M. Santamouris, M. Saliari, M. Assimakopoulos,Y. Caouris, The influence of air temperature and humidity on human thermalcomfort over the greater Athens area, Sustainable Cities and Society 10 (2014) 184-194.

[16] L. Peruzzi, F. Salata, A. De LietoVollaro, R. De LietoVollaro, The reliability of technological systems with high energy efficiency in residential buildings, Energy and Buildings 68(2014) 19-24.

[17] G. Battista, E. Carnielo, L. Evangelisti, M. Frascarolo, R. De Lieto Vollaro, Energy Performance and Thermal Comfort of a High Efficiency House: RhOME for denCity, Winner of Solar Decathlon Europe 2014, Sustainability 7(2015) 9681-9695

[18] F. Salata, A. De LietoVollaro, R. De LietoVollaro, A case study of technical and economic comparison among energy production systems in a complex of historic buildings in Rome, Energy Procedia 45(2014) 482-491.

[19] S. Bottillo, A. De LietoVollaro, G. Galli, A. Vallati, CFD modeling of the impact of solar radiation in a tridimensional urban canyon at different wind conditions, Solar Energy 102(2014) 212-222.

[20] S. Bottillo, A. De LietoVollaro, G. Galli, A. Vallati, Fluid dynamic and heat transfer parameters in an urban canyon, Solar Energy 99(2014) 1-10.

[21] S. Parizzotto, R. Lamberts, Investigation of green roof thermal performance intemperate climate: a case study of an experimental building in Florianopoliscity, Southern Brazil, Energy and Buildings 43 (2011) 1712-1722.

[22] A. Gagliano, M. Detommaso, F.Nocera, G.Evola, A multi-criteria methodology for comparing the energy andenvironmental behavior of cool, green and traditional roofs, Building and Environment 90 (2015) 71-81.sa
[23] M. Zinzi, E. Carnielo, S. Agnoli, Characterization and assessment of cool coloured solar protection devices for Mediterranean residential buildings application, Energy and Buildings 50(2012) 111-119.
[24] M. Zinzi, E. Carnielo, A. Federici, Preliminary studies of a cool roofs' energy-rating system in Italy, Advances in Building Energy Research 8-1 (2014) 84-96.
[25] D. Kolokotsa, C. Diakaki, S. Papantoniou, A. Vlissidis, Numerical and experimental analysis of cool roofs application on a laboratory building in Iraklion,Crete, Greece, Energy and Buildings55 (2012) 85-93.
[26] H. Akbari, R. Levinson, L. Rainer, Monitoring the energy use effects of cool roofs on California commercial buildings,Energy and Buildings37-10 (2005) 1007-1016.
[27] E.Carnielo, M.Zinzi, Optical and thermal characterisation of cool asphalts to mitigate urban temperatures and building cooling demand, Building and Environment 60 (2013) 56-65.
[28] M.Santamouris, A.Synnefa, T.Karlessi, Using advanced cool materials in the urban built environment to mitigate heat islands and improve thermal comfort conditions, Solar Energy 85-12 (2012)3085-3102.
[29] A.M. Coutts, J. Beringer, N.J. Tapper, Impact of Increasing Urban Density on Local Climate: Spatial and Temporal Variations in the Surface Energy Balance in Melbourne, Australia, School of Geography and Environmental Science, Monash University, Melbourne, Victoria, Australia.
[30] C. Rinner, M. Hussain, Toronto's Urban Heat Island—Exploring the Relationship between Land Use and Surface Temperature, Department of Geography, Ryerson University, Remote Sensing, 3 (6) (2011), 1251-1265
[31] L.D. Frank, P.O. Engelke, The Built Environment and Human Activity Patterns: Exploring the Impacts of Urban Form on Public Health, Journal of Planning Literature, 16 (2) (2001), 202-2018.
[32] ENVI-met website: http://envi-met.com/
[33] M.F. Shahidan, P.J. Jones, J. Gwilliam, E.Salleh, An evaluation of outdoor and building environment cooling achieved through combination modification of trees with ground materials, Building and Environment 58 (2012)245-257.
[34] W.T.L. Chow, A.J.Brazel, Assessing xeriscaping as a sustainable heat island mitigation approach for a desert city,Building and Environment 47 (2012)170-181.
[35] E.L. Krüger, F.O. Minella, F. Rasia, Impact of urban geometry on outdoor thermal comfort and air quality from field measurement in Curitiba, Brazil,Building and Environment 46 (2011)621-634.
[36] RAYMAN website:http://www.urbanclimate.net/rayman/
[37] C. Ketterer, A. Matzarakis, Human-biometeorological assessment of the urban heat island in a city with complex topography – The case of Stuttgart, Germany, Urban Climate 10 (2014) 573-584.
[38] C.J. Willmott, Some Comments on the Evaluation of Model Performance, Bulletin of the American Meteorological Society 63-11 (1981) 1309-1313.
[39] G. Jendritzky, R. Dear, G. Havenith, UTCI—Why another thermal index?, International Journal of Biometeorol 56-3(2012) 421-428.
[40] M. Despotovic, V. Nedic, D. Despotovic, S Cvetanovic, Review and statistical analysis of different global solar radiation sunshine models, Renewable and Sustainable Energy Reviews 52(2015) 1869-1880.
[41] International Union of Physiological Sciences, Thermal Commission, Glossary of terms for thermal physiology, Journal of Thermal Biology 28-1(2003) 75-106.

Figure 1. View of the "ex Mercati Generali" area and monitoring point.

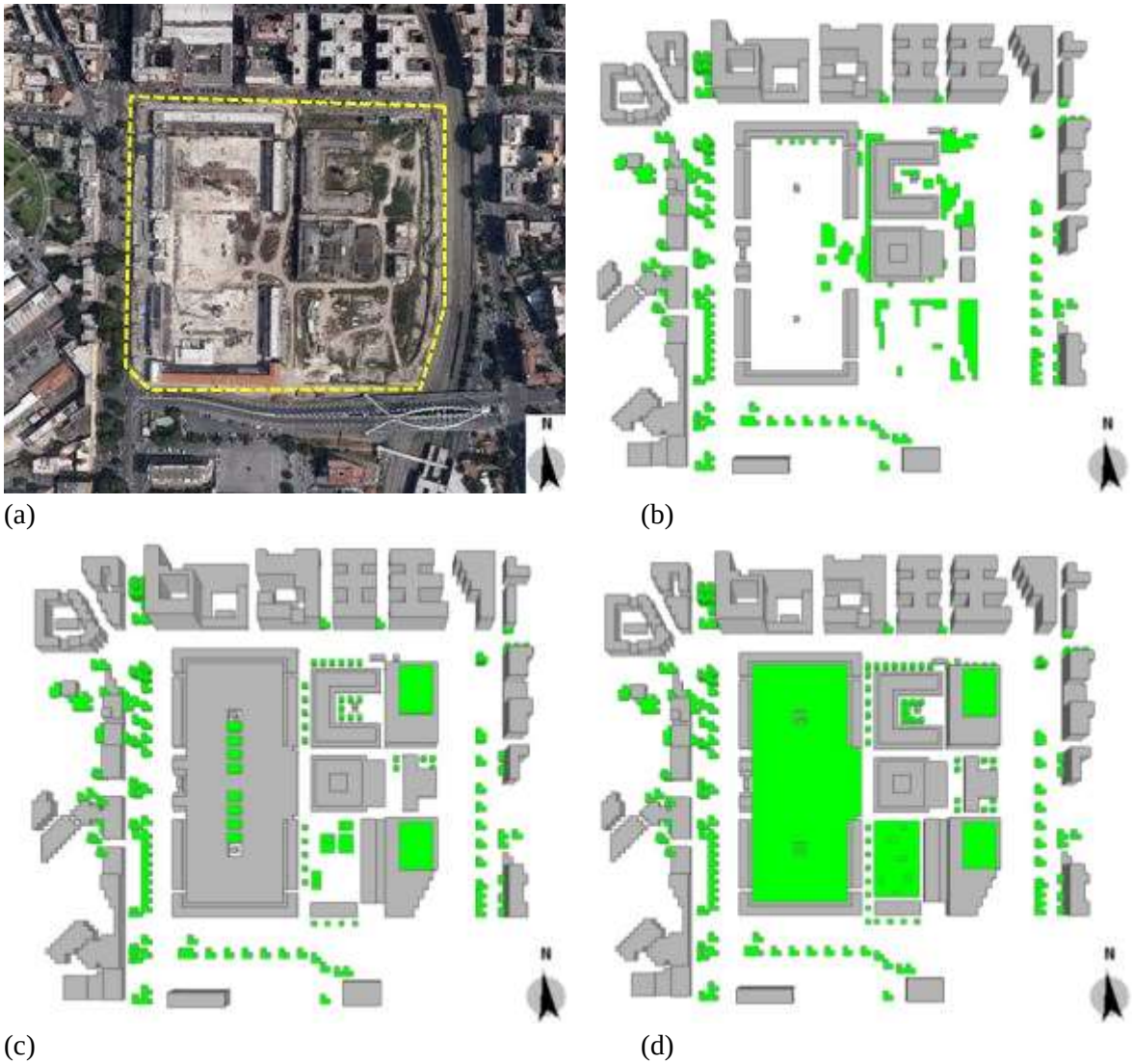

Figure 2. Micro-scale models: **(**a) "ex Mercati Generali" aerial view; (b) *ante-operam*; (c) *post-operam*; (d) *final-post-operam*.

Figure 3. Calibration receptor RC at the "ex Mercati Generali" area and *ante-operam* model.

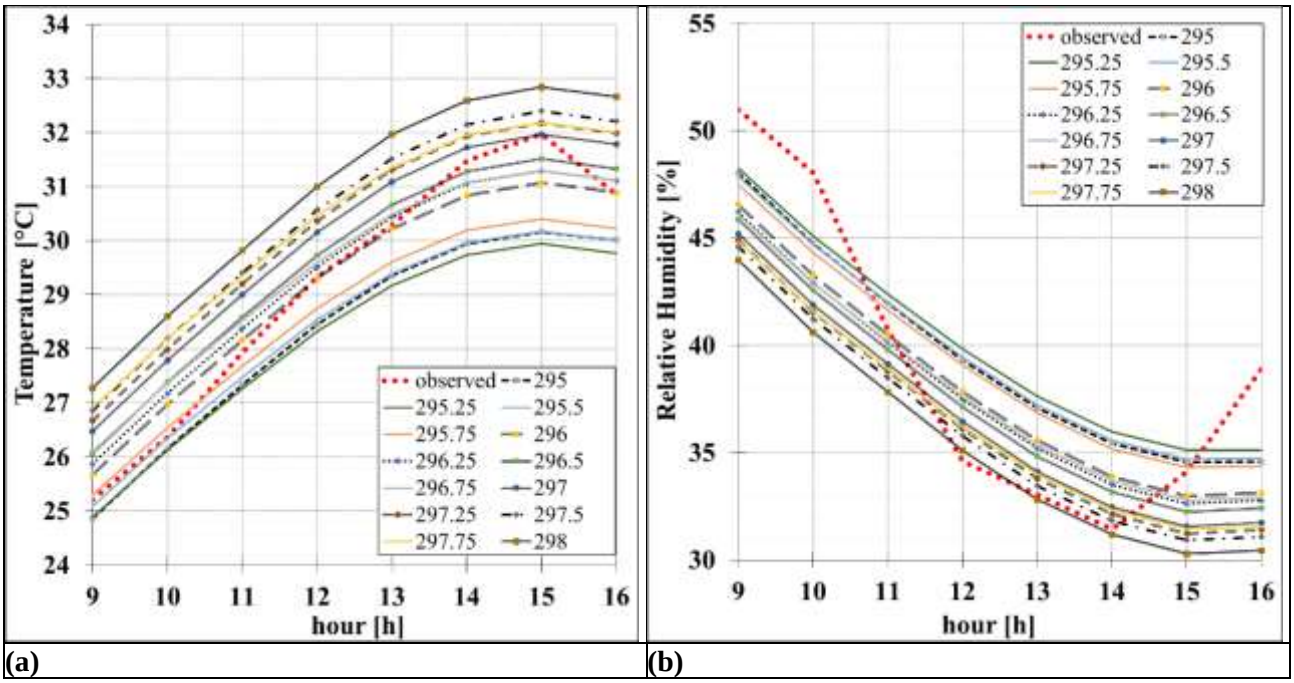

(a) **(b)**

Figure 4. Trend of observed and the model-predicted air temperature (a)and relative humidity (b) varying the model initial potential temperature of the atmosphere.

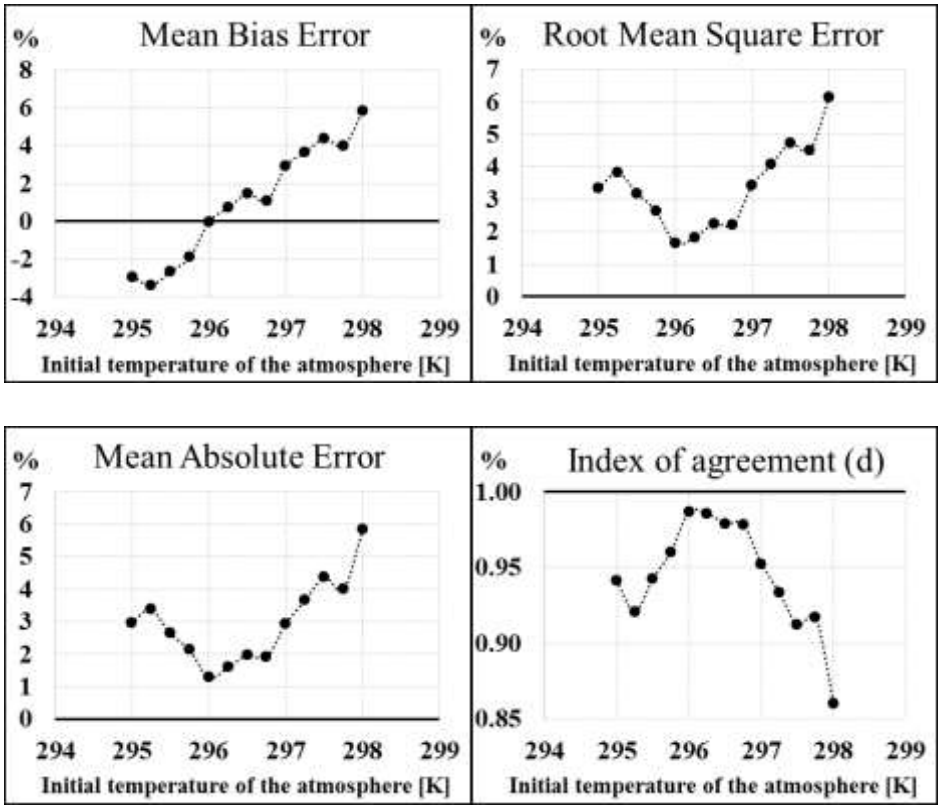

Figure 5. Simulation error between the observed and the model-predicted air temperature values varying the model initial potential temperature of the atmosphere.

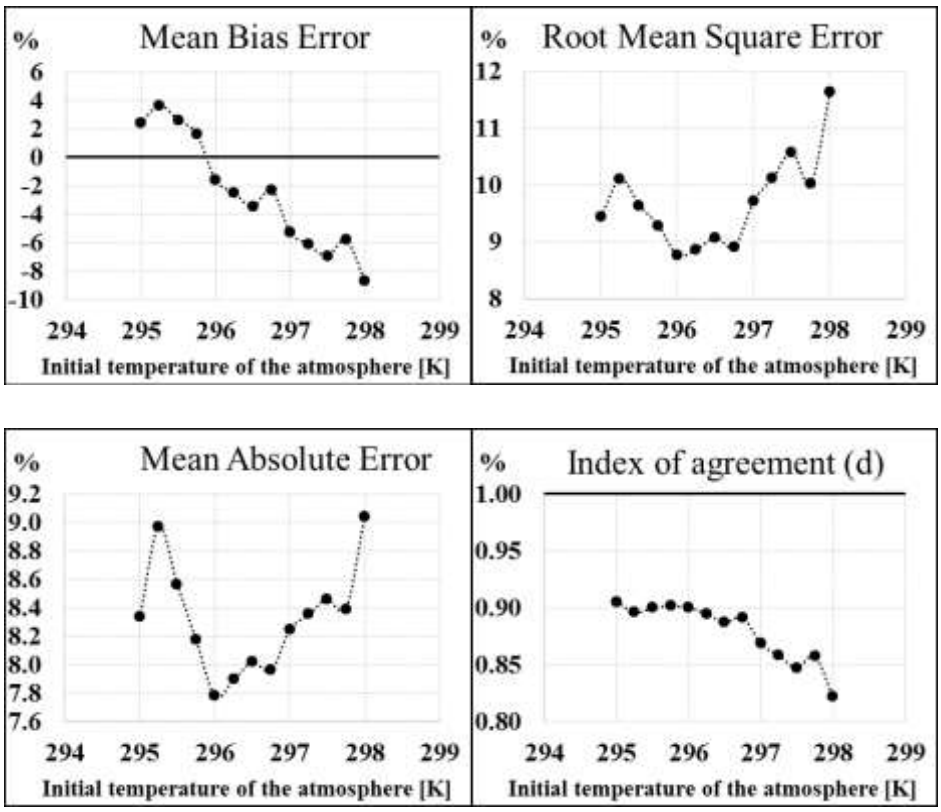

Figure 6. Simulation error between the observed and the model-predicted relative humidity values varying the model initial potential temperature of the atmosphere.

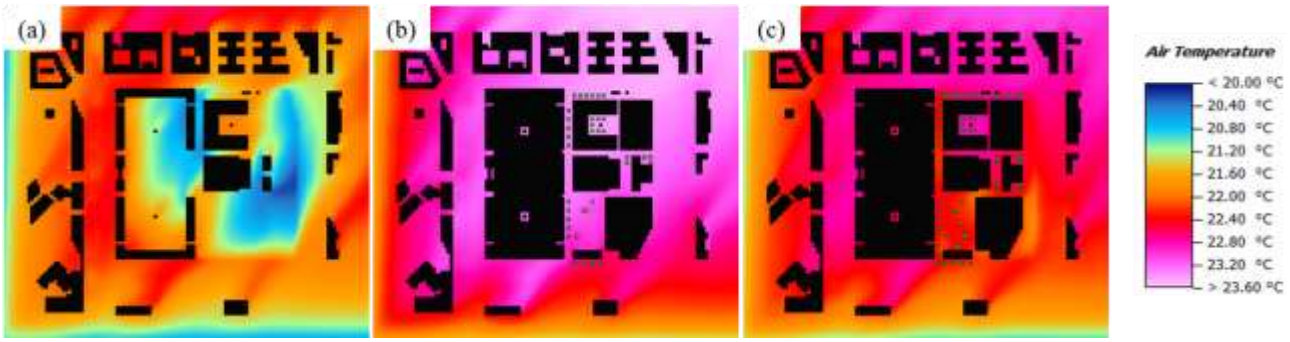

Figure 7. Thermal map of the "ex Mercati Generali area on July 16th at 6:00 AM 1.5 m height: (a) *ante-operam* model; (b) *post-operam* model; (c) *final-post-operam* model.

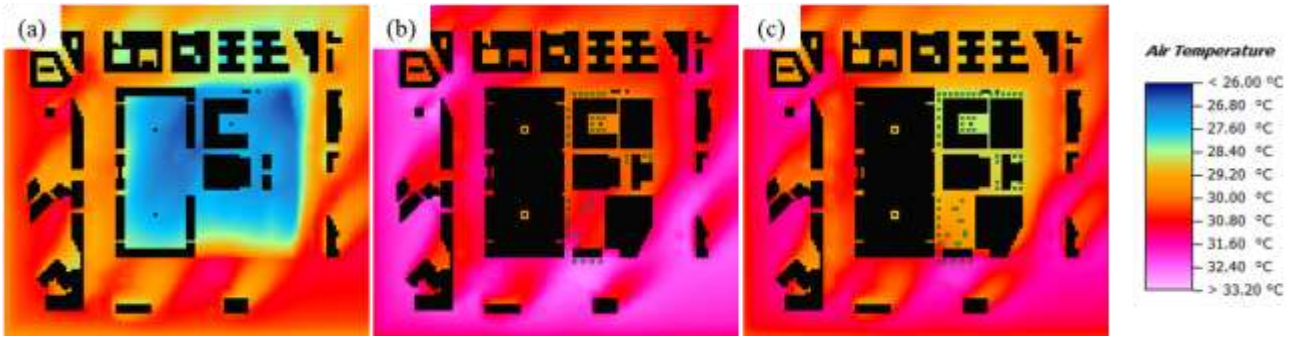

Figure 8. Thermal map of the "ex Mercati Generali area on July 16th at 12:00 AM 1.5 m height: (a) *ante-operam* model; (b) *post-operam* model; (c) *final-post-operam* model.

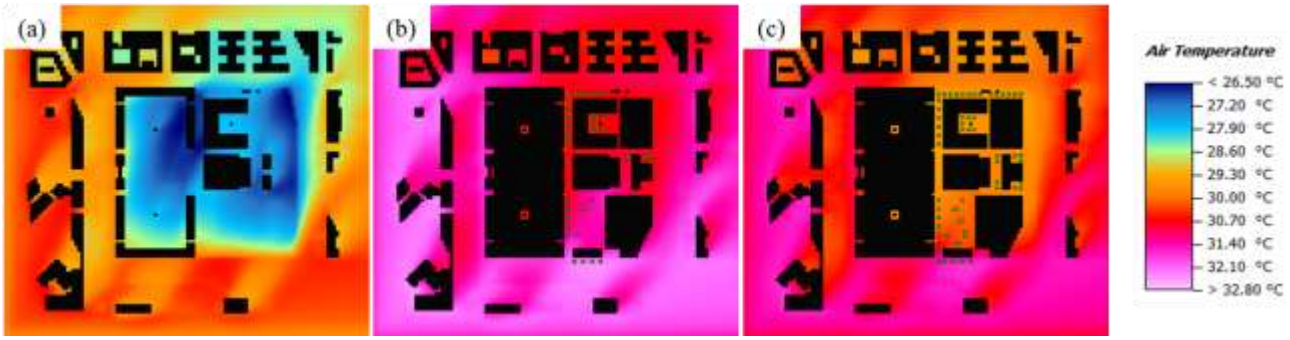

Figure 9. Thermal map of the "ex Mercati Generali area on July 16th at 6:00 PM 1.5 m height: (a) *ante-operam* model; (b) *post-operam* model; (c) *final-post-operam* model.

Figure 10: Investigation point of vertical temperature profiles.

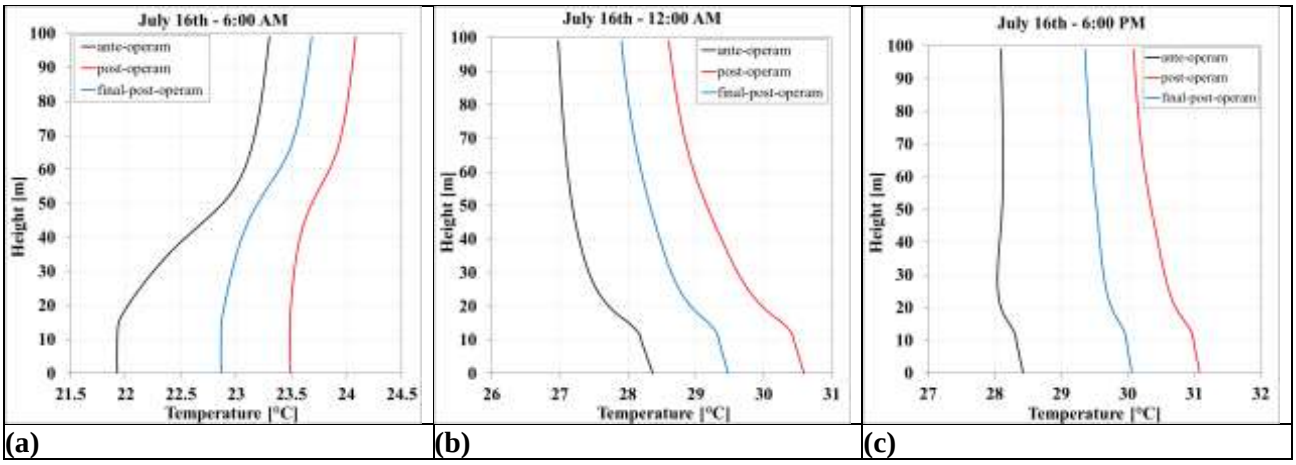

Figure 11: Vertical temperature profiles in the investigation point on July 16th: (a) at 6:00 AM; (b) at 12:00 AM; (c) at 6:00 PM.

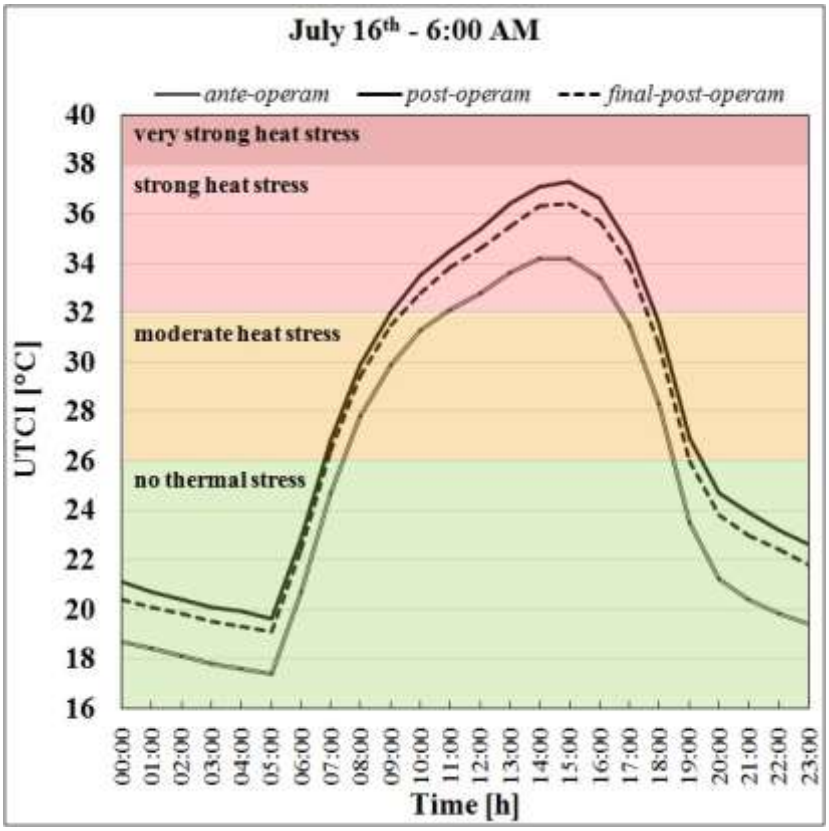

Figure 12: Universal Thermal Climate Index (UTCI) in the investigation point on July 16th.

Table 1. Input parameters in the numerical analysis

Parameter	Value
Atmosphere temperature at 2500 m [K]	used for model validation
Wind Speed [m/s]	2.5
Wind Direction [°]	225 (South-West)
Specific Humidity at 2500 m [$g_{water\ vapor}/kg_{air}$]	7
Relative Humidity at 2 m [%]	65
Roughness length at measurement site [m]	0.01

Table 2. Solar and thermal properties of construction materials used in the three urban models.

Urban Models	Soil Albedo [-]	Wall Albedo [-]	Roof Albedo [-]	Wall Thermal Conductivity [W/mK]	Roof Thermal Conductivity [W/mK]
Ante-operam	0.35	0.30	0.30	1.30	1.30
Post-operam	0.20	0.30	0.30	1.30	1.30
Final-post-operam	0.75	0.75	0.75	1.30	1.30

Table 3. Statistical indices for the initial temperature of the atmosphere equal to 296 K.

Variable	MBE [%]	RMSE [%]	MAE [%]	d [%]
Air temperature	-0.01	1.64	1.28	0.99
Air humidity	-1.57	8.77	7.78	0.90

Table 4. UTCI Assessment Scale: UTCI categorized in terms of thermal stress.

UTCI (°C) range	**Stress Category**
above +46	extreme heat stress
+38 to +46	very strong heat stress
+32 to +38	strong heat stress
+26 to +32	moderate heat stress
+9 to +26	no thermal stress
+9 to 0	slight cold stress
0 to -13	moderate cold stress
-13 to -27	strong cold stress
-27 to -40	very strong cold stress
below -40	extreme cold stress